Lattice dynamics of a rotor-stator molecular crystal: Fullerene-cubane C 60 · C 8 H 8

Colin Bousige, Stéphane Rols, Julien Cambedouzou, Bart Verberck, Sándor Pekker, Éva Kováts, Gábor Durkó, István Jalsovsky, Eric Pellegrini, Pascale Launois

▶ **To cite this version:**

Colin Bousige, Stéphane Rols, Julien Cambedouzou, Bart Verberck, Sándor Pekker, et al.. Lattice dynamics of a rotor-stator molecular crystal: Fullerene-cubane C 60 · C 8 H 8. Physical Review B: Condensed Matter and Materials Physics (1998-2015), 2010, 82 (19), 10.1103/PhysRevB.82.195413 . hal-01611940

HAL Id: hal-01611940
https://hal.science/hal-01611940

Submitted on 6 Oct 2017

HAL is a multi-disciplinary open access archive for the deposit and dissemination of scientific research documents, whether they are published or not. The documents may come from teaching and research institutions in France or abroad, or from public or private research centers.

L'archive ouverte pluridisciplinaire **HAL**, est destinée au dépôt et à la diffusion de documents scientifiques de niveau recherche, publiés ou non, émanant des établissements d'enseignement et de recherche français ou étrangers, des laboratoires publics ou privés.

PHYSICAL REVIEW B **82**, 195413 (2010)

Lattice dynamics of a rotor-stator molecular crystal: Fullerene-cubane $C_{60}\cdot C_8H_8$

Colin Bousige,[1,2] Stéphane Rols,[1] Julien Cambedouzou,[2] Bart Verberck,[2,3] Sándor Pekker,[4] Éva Kováts,[4] Gábor Durkó,[5] István Jalsovsky,[5] Éric Pellegrini,[1] and Pascale Launois[2]

[1]*Institut Laue Langevin, F-38042 Grenoble, France*

[2]*Laboratoire de Physique des Solides, UMR CNRS 8502, Université Paris-Sud, F-91405 Orsay, France*

[3]*Departement Fysica, Universiteit Antwerpen, Groenenborgerlaan 171, B- 2020 Antwerpen, Belgium*

[4]*Research Institute for Solid State Physics and Optics, Hungarian Academy of Sciences, P.O. Box 49, H-1525 Budapest, Hungary*

[5]*Department of Organic Chemistry, Eötvös Loránd University, P.O. Box 32, H-1518 Budapest, Hungary*

(Received 30 July 2010; published 8 November 2010)

The dynamics of fullerene-cubane ($C_{60}\cdot C_8H_8$) cocrystal is studied combining experimental [x-ray diffuse scattering, quasielastic and inelastic neutron scattering (INS)] and simulation (molecular dynamics) investigations. Neutron scattering gives direct evidence of the free rotation of fullerenes and of the libration of cubanes in the high-temperature phase, validating the "rotor-stator" description of this molecular system. X-ray diffuse scattering shows that orientational disorder survives the order/disorder transition in the low-temperature phase, although the loss of fullerene isotropic rotational diffusion is featured by the appearance of a 2.2 meV mode in the INS spectra. The coupling between INS and simulations allows identifying a degeneracy lift of the cubane librations in the low temperature phase, which is used as a tool for probing the environment of cubane in this phase and for getting further insights into the phase transition mechanism.

DOI: 10.1103/PhysRevB.82.195413 PACS number(s): 78.70.Nx, 61.05.cp, 81.05.ub

I. INTRODUCTION

The chemistry of fullerenes includes an almost infinite collection of inclusion compounds. The large voids existing between the fullerenes in their crystalline structure allow intercalation of a large spectrum of molecules or atomic species. This results in a wide range of interesting effects, from chemical reactions [polymerization of the fullerenes in $Li_4\cdot C_{60}$ (Ref. 1)] to superconductive behavior [$Cs_3\cdot C_{60}$ (Ref. 2)]. In particular, it has been shown that the intercalation of small diatomic molecules and rare gases (N_2, O_2,[3–5] CO,[6] Ar, Kr, Xe,[7]…) sensitively modifies the phase diagram of C_{60}.

The C_{60} phase diagram is roughly characterized by a first-order transition at $T_c \simeq 260$ K from a face-centered cubic (fcc) orientationaly disordered phase ("orientational gas" $Fm\bar{3}m$) to an orientationaly ordered simple cubic phase ($Pa\bar{3}$).[8] This ordered phase is described by a two-state model where the molecules are found in two energetically nearly degenerate orientations. These two states, adopted at random, have a temperature-dependent population, so that a certain disorder remains concerning the C_{60} orientation in the $Pa\bar{3}$ phase. At $T_g \simeq 90$ K, the system undergoes a glass transition in which it is frozen in an orientational glass state.[9] It was found that the insertion of inert molecules inside the C_{60} network significantly lowers the order-disorder transition temperature T_c (Refs. 3–7) (see Fig. 6). The inserted guests were therefore described as molecular lubricants. In addition, the insertion resulted in the disappearance of the glass transition.

In this paper, we present a study of the dynamics of a fullerene-cubane $C_{60}\cdot C_8H_8$ cocrystal, which was synthesized for the first time by Pekker *et al.*[11] The interest of this model system stands in the complex molecular nature of the cocrystal, where molecules of icosahedral and cubic symmetries interact. The fcc unit cell of the disordered phase is represented in Fig. 1, with the fullerene molecules occupying the corners and the centers of the cubic cell while the cubane molecules are located at the octahedral sites. The mixture of symmetry of the constituent molecules is reflected in their dynamics, as at room temperature the C_{60} molecules rotate freely while the cubanes remain static: the $C_{60}\cdot C_8H_8$ cocrystal appears as a *molecular rotor-stator system*.

Since its discovery, the structure of fullerene-cubane cocrystal has been extensively studied by Raman and infrared spectroscopies,[12,13] ^{1}H-nuclear magnetic resonance,[14] x-ray diffraction and calorimetry,[11,15] which allowed to produce the pressure-temperature (P,T) "reaction map" of this crystal.[13] These studies showed that fullerene-cubane polymerizes into a very stable covalent derivative in which decomposed cubanes form covalent bonds with adjacent fullerenes[13,16] above 500 K.

Alike the other fullerene insertion compounds, the fullerene-cubane cocrystal undergoes a first-order transition at $T_c \simeq 140$ K, attributed to the orientational ordering of the

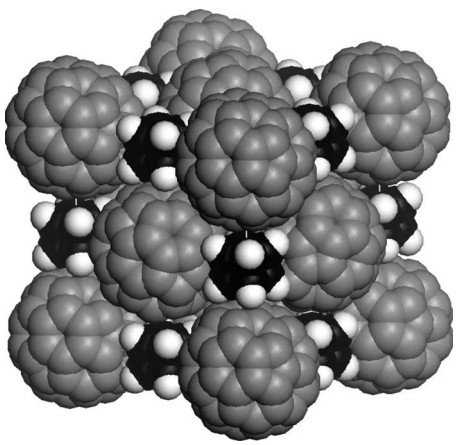

FIG. 1. Visualization of the fullerene-cubane fcc lattice.

 ©2010 The American Physical Society

C_{60} molecules. The low-temperature phase was indexed as orthorhombic[11] but its space group, requiring the knowledge of the fullerene orientations, is still unknown.

Until now, little attention was given to the dynamics of the molecules around the transition at 140 K, which could give precious information in order to understand the transition mechanism as well as the state of the system at low temperature. For this reason, we have performed x-ray diffuse scattering (XRDS) studies of a fullerene-cubane single crystal around the transition temperature. This allowed us to show that a strong C_{60} orientational disorder persists below the transition. This study is detailed in the first part of this paper.

In addition, we have conducted inelastic neutron scattering (INS) measurements on a powder of fullerene-cubane around T_c. INS is the preferred method to study low-frequency vibrations, and thus provides precious information on the intermolecular dynamics of both fullerenes and cubanes. The experimental data are interpreted by means of molecular dynamics (MD) simulations and reported in the second part of this paper.

II. EXPERIMENTAL

A. Sample preparation

Two samples were used for these experiments: a small monocrystal (platelet shape sample as described in Ref. 11, with a characteristic size in the platelet plane being of about 200 μm), and a 200 mg powder. Cubane was synthesized by the method of Eaton.[17] $C_{60}\cdot C_8H_8$ cocrystals were prepared in the form of microcrystalline powder and monocrystals by the methods described in details in Ref. 11. It consists of dissolving a C_{60} powder in toluene, and filtering it before adding excess amount of cubane to the solution. In order to get microcrystals, toluene was removed by distillation in a rotary evaporator. For producing single crystals, isopropyl alcohol was layered to the toluene solution, and at room temperature $\sim$100–200 μm crystals were grown within a week. Finally all the crystals were washed with ethanol for removing the residual cubane.

B. X-ray diffractometer

We have performed single crystal x-ray scattering experiments at $\lambda=1.5418$ Å on a $C_{60}\cdot C_8H_8$ platelet-shaped single crystal.

Measurements were performed in transmission geometry, using a cylindrical image plate as a detector (fixed crystal-fixed detector geometry). The temperature was controlled using a displex, allowing the (30–300 K) temperature range to be covered. The collimator as well as the beam stop were placed within the displex beryllium cell, which allowed us to minimize parasitic diffraction from the cell.

C. INS spectrometer

INS measurements were performed on a 200 mg fullerene-cubane powder using the IN4C spectrometer, which is a time of flight spectrometer mounted on the thermal source at the ILL. Incident neutrons with wavelengths 2.7, 1.65, and 1.5 Å were used in elastic time focusing conditions. This allowed us to study the respective following energy ranges:[18] 0 to 8 meV with 0.5 meV resolution, 0 to 25 meV with 1.25 meV resolution, and 0 to 50 meV with 1.5 meV resolution. The measurements, performed at different temperatures between 300 and 10 K, were corrected for the scattering of the sample holder and normalized to vanadium [see Figs. 3, 4(a), and 5]. The signal was transformed into either the so-called generalized density of states $[\mathrm{GDOS}(\omega)]$, susceptibility $[\chi''(\omega)/\omega]$ or into the dynamical structure factor $[S(Q,\omega)]$, depending on the most convenient representation.[20] Note that we will call "susceptibility" the imaginary part of the susceptibility divided by the frequency. The generalized vibrational density of states can be derived in an extensive (0–200 meV) energy scale using a relatively large neutron incident wavelength (here we used 3 Å corresponding to $\sim$9 meV incident energy) in up-scattering mode (e.g., anti-Stokes scattering) and at relatively high temperature (300 K). The unavoidable deterioration of the energy resolution with increasing energy transfer can be minimized by time focusing in the inelastic range, a condition requiring that the Fermi chopper spins at high speed. We chose a Fermi speed of 13 000 RPM and conditions so that frame overlap could be avoided.

In a neutron experiment, the quantity measured is proportional to the so-called differential scattering cross section $\frac{\partial^2\sigma}{\partial\Omega\partial E}$ which gives the number of incident neutrons with wave vector $\vec{k}_i$ scattered by the sample in a solid angle $\partial\Omega$ around the solid angle $\vec{\Omega}$ and with an energy range ∂E around E (i.e., having a scattered wave vector $\vec{k}_f$). Due to the peculiar neutron-nucleus interaction, this quantity can be split into a *coherent* and an *incoherent* cross section, so that it can be expressed as

$$\frac{\partial^2\sigma}{\partial\Omega\,\partial E}=\left(\frac{\partial^2\sigma}{\partial\Omega\,\partial E}\right)_{coh}+\left(\frac{\partial^2\sigma}{\partial\Omega\,\partial E}\right)_{inc}$$

with the relative ratio between coherent and incoherent intensity being a function of the chemical and isotopic composition of the sample. A $C_{60}\cdot C_8H_8$ powder contains only carbon and hydrogen atoms in natural isotopic ratio. The incoherent cross section is written

$$\left(\frac{\partial^2\sigma}{\partial\Omega\,\partial E}\right)_{inc}\propto\sum_{\alpha=\{C,H\}}\sigma^{\alpha}_{inc}S^{\alpha}_{inc}(\vec{Q},\omega),\qquad(1)$$

where α runs over the atomic species (here carbon and hydrogen) and σ^{α}_{inc} refers to the incoherent cross section associated with this type of atom. In our case, the carbon incoherent cross section is negligible compared to that of hydrogen ($\sigma^{C}_{inc}=0.001$ barn and $\sigma^{H}_{inc}=80.26$ barn), such that the incoherent cross section will be entirely due to scattering by hydrogen atoms. For a powder of fullerene-cubane, one can write that

$$\left(\frac{\partial^2\sigma}{\partial\Omega\,\partial E}\right)_{inc}=\frac{k_f}{k_i}\frac{\sigma_H}{4\pi}S^{H}_{inc}(Q,\omega)\qquad(2)$$

while the coherent part of the total cross section will be dominated by carbon atoms ($\sigma^{C}_{coh}=5.551$ barn and σ^{H}_{coh}

=1.756 barn). The inelastic "one-phonon" incoherent scattering function $S_{inc}^{\pm 1}(\vec{Q},\omega)$ can be obtained by developing $S_{inc}^{H}(\vec{Q},\omega)$ in terms of the atomic displacement (considered small compared to the neutron wavelength) and considering only the second term of the development, the first being related to the elastic scattering (see, for example, Ref. 21). Within the harmonic approximation, it can be shown that this term is expressed as

$$S_{inc}^{\pm 1}(Q,\omega) \propto e^{-2W(Q)} \frac{Q^2}{\omega} n^{\pm}(\omega,T) G(\omega), \tag{3}$$

where the exponent $\pm$ refers to neutron energy gain (+, anti-Stokes) or neutron energy loss (−, Stokes) scattering processes. Q is the norm of the scattering vector, $n^{\pm}(\omega,T)$ the Bose population factor $(n^{-}=n^{+}+1)$, $2W(Q)=Q^2\langle u^2\rangle$ the Debye-Waller factor, $\langle u^2\rangle$ the total mean squared displacement, and $G(\omega)$ the GDOS expressed as

$$G(\omega) = \sum_{j,\vec{q}} \delta[\omega - \omega_j(\vec{q})] \sum_{\alpha} \frac{\sigma_{inc}^{\alpha}}{m_{\alpha}} |\vec{e}_{\alpha}(j,\vec{q})|^2, \tag{4}$$

where $(j,\vec{q})$ denotes the phonon modes of frequency $\omega_j(\vec{q})$ and polarization vector $\vec{e}(j,\vec{q})=\Sigma_{\alpha}\vec{e}_{\alpha}(j,\vec{q})$ while σ_{inc}^{α} and m_{α} stands, respectively, for the incoherent cross section and the mass of the atom α in the unit cell. In the case of fullerene-cubane, the sum over α reduces to the sum over the hydrogen atoms of the cubane in the unit cell, due to the dominant factor σ_{inc}^{H}/m_H. The GDOS $G(\omega)$ can be obtained by measuring $S_{inc}^{\pm 1}(Q,\omega)$ at a fixed energy transfer $\hbar\omega$ and for a set of Q values. Then, from Eq. (3), the quantity

$$f(Q,\omega) = \ln\left[\frac{\omega S_{inc}^{\pm 1}(Q,\omega)}{Q^2 n^{\pm}(\omega,T)}\right] = \ln[G(\omega)] - Q^2\langle u^2\rangle \tag{5}$$

can be plotted as a function of Q^2 and fitted to a line. The constant term allows $G(\omega)$ to be derived.

In conclusion, for a powder sample and using a time-of-flight machine equipped with a multidetector such as IN4C, the signal measured will be essentially originating from incoherent scattering by the hydrogen atoms at the surface of the cubane molecules. The coherent signal from the carbon atoms, and therefore the C_{60} dynamics, will be measurable only in the frequency ranges where cubane modes are absent. They will appear as small Q-dependent contributions in the spectrum, the most intense coherent feature being the C_{60} rotation and libration as we will show later.

D. Numerical simulations

X-ray scattering simulations were performed by using a homemade program, allowing one to take into account the geometry of the experiment (crystal orientation, distance between the crystal and the detector, cylindrical shape of the detector, etc.) and to calculate, for each pixel on the detector, Bragg and diffuse scattering intensities within structural models defined in the program.[22] The calculated intensities are represented in two-dimensional areas with the same shape and size as the detector to allow for an easy visual comparison.

Neutron functions were calculated using MD simulations. They were performed using the module *Discover* supplied by *Materials Studio*.[23] The model was composed of a supercell containing $2\times2\times2$ cubic lattice cells, resulting in a total of 32 fullerenes and 32 cubanes. We used the semi-*ab initio* force field *COMPASS*, and the trajectories issued from the *NVE* simulations were treated using the NMOLDYN software.[24] In particular, this software computes the velocity autocorrelation function from a MD trajectory which is linked to the GDOS by a time Fourier transformation. Moreover it allows performing group selections and transforming MD trajectories into rigid body trajectories (RBT) for which only the translation and rotation degree of freedom of each molecule as a whole are computed. The neutron functions issued from these calculations are further convoluted with a resolution function allowing for a direct comparison with the experimental data.

III. EXPERIMENTAL RESULTS

A. Diffuse scattering

X-ray scattering is a most useful tool for the investigation of the structure of crystalline materials, as it reveals the mean crystallographic structure through diffraction and it measures the degree of disorder relative to the mean structure through diffuse scattering.

Figure 2(a) shows the x-ray scattering pattern of a $C_{60}\cdot C_8H_8$ platelet-shaped crystal recorded at room temperature. The platelet was placed perpendicular to the incident beam. At room temperature, the Bragg spots show a sixfold symmetry compatible with the fcc structure proposed in Ref. 11, provided that a (111) mirror twin is considered. Such twinning effects are rather common in fcc crystals. Calculation of Bragg peak intensities within the structural model of Ref. 11, which assumes complete orientational disorder of C_{60} molecules—approximated as homogeneous spheres—is shown in Fig. 2(c) in good agreement with Fig. 2(a). Apart from Bragg reflections, Fig. 2(a) reveals a diffuse scattering halo at 3.3 $Å^{-1}$. It is characteristic of complete orientational disorder of the C_{60} molecules,[25] as is shown for instance in Ref. 22 for pure C_{60} single crystal. It appears distorted in Fig. 2(a) because of the cylindrical shape of the image plate but it corresponds in fact to an isotropic halo. Diffuse scattering calculated for complete orientational disorder of the C_{60} molecules is drawn in Fig. 2(c), using Eq. (15) in Ref. 22. It should be noticed that the intra-Brillouin zone modulations of the diffuse ring observed at room temperature for pure C_{60} crystal[22] are not observed in the case of $C_{60}\cdot C_8H_8$, neither at room temperature nor at lower temperatures, close to the transition temperature ($T_c\simeq 140$ K). In pure C_{60}, such modulations were due to intermolecular orientational correlations.[26] In fullerene-cubane, topological recognition between the convex surface of fullerenes and the concave surfaces of cubanes act as bearings between the fullerene molecules and thus interfullerene correlations are much smaller. It is consistent with the lowering of the transition temperature from 260 K in pure C_{60} to 140 K in $C_{60}\cdot C_8H_8$.

In conclusion, x-ray diffraction and diffuse scattering data at room temperature both point toward total C_{60} orientational

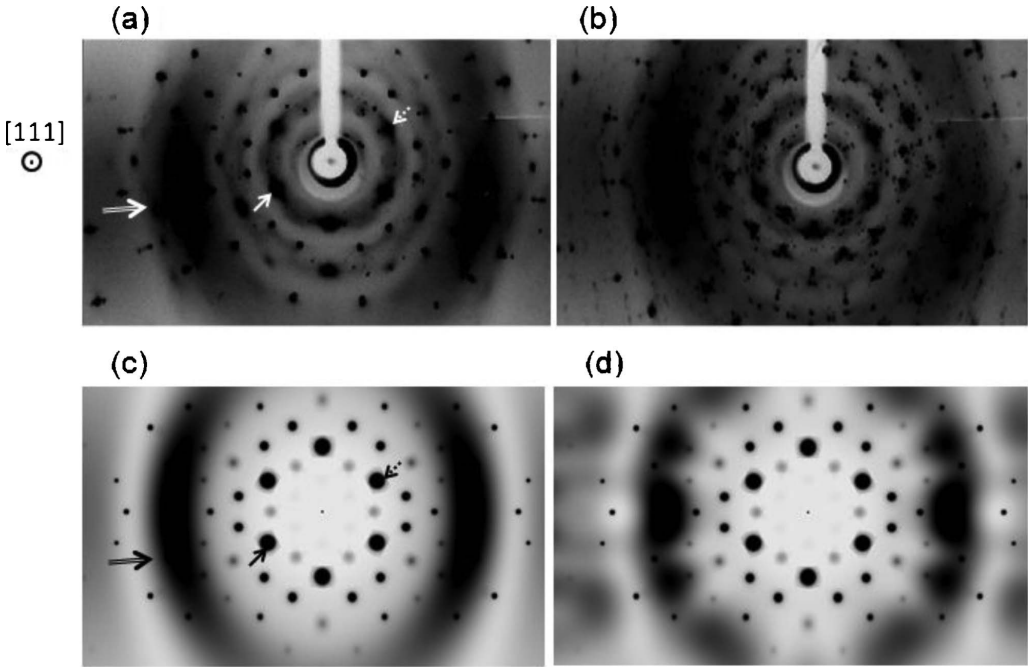

FIG. 2. X-ray scattering pattern of a $C_{60}\cdot C_8H_8$ crystal, recorded on a cylindrical image plate (a) at room temperature and (b) at 120 K. The [111] cubic axis is parallel to the x-ray beam (perpendicular to the pattern). Simulations are reported in (c) and (d) using the structural parameters refined in Ref. 11 to calculate Bragg peak intensities. Diffuse scattering intensity is calculated assuming that molecules take all orientations in (c) or that they can take 24 orientations in (d), as discussed in the text. Simulations are performed assuming that the crystal contains in identical ratio the "parent" crystal and its (111) mirror twin. Simple arrows point toward the $1,-3,1$ diffraction peak of the parent crystal and dotted arrows point toward the same peak for the twin crystal. Double arrows point toward the diffuse scattering halo around 3.3 $Å^{-1}$ characteristic of C_{60} orientational disorder.

disorder. However, it is not possible on the basis of x-ray scattering to discriminate between static and dynamic disorder. The dynamical character of this disorder is discussed in the inelastic neutron scattering section hereafter.

When the temperature is lowered below 140 K, the appearance of new Bragg reflections testifies to a structural transition to a less symmetric structure, as is illustrated by the diffraction pattern measured at 120 K shown in Fig. 2(b). This phase transition is reported as an orientational-ordering phase transition (see, e.g., Ref. 11). However, surprisingly, appearance of new Bragg reflections is not concomitant with measurable modifications of the diffuse scattering halo around 3.3 $Å^{-1}$, which has similar shape in Figs. 2(a) and 2(b). Diffuse scattering intensities, normalized to counting time, are also the same at room temperature and at 120 K within experimental precision (10–20 %). One would have expected the disappearance of the diffuse scattering halo if the C_{60} molecules were completely ordered below the transition or at least modification of the distribution of intensity in the diffuse halo if molecules presented lower orientational disorder. In the case of pure C_{60} for instance, where two different types of orientations coexist below the transition,[8] one observes modulations of the diffuse halo.[27] As detailed in Ref. 27, these modulations are well accounted for within the standard formalism used in the case of binary alloys with a Laue formula where atomic form factors are replaced by molecular form factors for the different orientations. The rapid modulations of the molecular form factor (large size of C_{60}) give rise to pronounced modulations of the halo. Similar results are obtained in the case of fullerene-biphenyl and of fullerene-tetraphenylphosphonium bromide compounds,[28,29] where different molecular orientations are also present. To try to explain the observed diffuse scattering in the low-temperature phase of fullerene-cubane, we have calculated the diffuse scattering for 24 different orientations of the C_{60} molecules. It corresponds to partial orientational ordering with respect to the high-temperature phase where molecules could take all orientations with the same probability. The structure of the low-temperature phase of fullerene-cubane being unknown, it was not possible to generate equivalent orientations using its symmetry operations. We have thus used the symmetry operations of the high-temperature phase. One orientation was chosen by rotating a molecule in standard orientation, with its twofold axes along the cubic axes, by the Euler matrix (Euler angle values being arbitrarily taken equal to 8°, 31°, and 17°) from which the other configurations were deduced by the symmetry operations of the high-temperature cubic phase. Calculated diffuse scattering pattern is reported in Fig. 2(d). Comparison between Fig. 2(c), where molecules are assumed to take all orientations and Fig. 2(d) shows slight modulations of the halo at 3.3 $Å^{-1}$. One can also extrapolate from this comparison that modulations will be smoothed, diffuse scattering hence looking more like a diffuse halo, if there are large amplitude fluctuations around the different preferential orientations.

B. Inelastic neutron scattering

The GDOS measured at 300 K for the powder of fullerene-cubane is shown in Fig. 3. It features different fre-

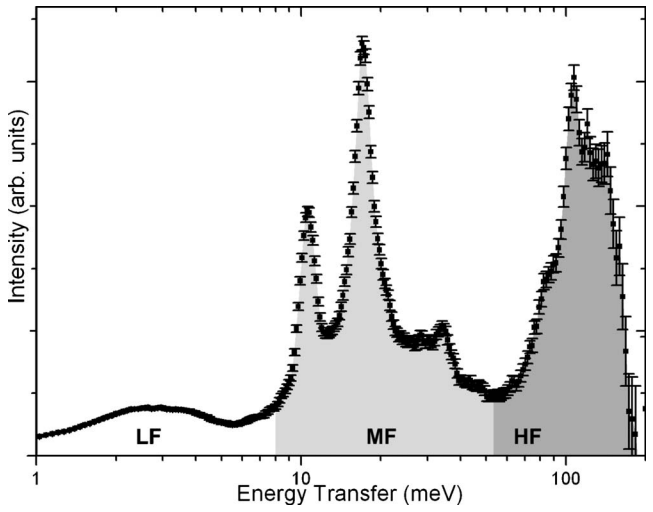

FIG. 3. Generalized density of states (GDOS) measured at 300 K and 3 Å. We consider three zones labeled low, mid, and high frequencies. Features at HF are mainly due to internal vibrations of cubanes (intense features from 75 meV up to 200 meV). Small peaks attributable to fullerene vibrations are visible (the H_g vibration is visible at 33 meV). The two intense peaks in the MF region are due to cubanes intermolecular motions. The LF region shows a featureless intensity, associated to a quasielastic signal originating from slow reorientations of fullerenes.

quency domains—or bands—distributed over a broad frequency range and separated by "gaps." A high-frequency band (HF), having a maximum intensity at 100 meV, extends from 55 meV up to 170 meV. A medium frequency (MF) band, which is composed essentially of two strong peaks located at 11.0 and 17.8 meV with a smaller component located at 33 meV, is observed from 8 meV up to 55 meV. Finally, the lower frequency band (LF) shows a broad and featureless component extending up to 8 meV.

The total spectrum of a molecular crystal is generally split into such bands, each being characteristic of a certain type of bonding between atoms or molecules. In general, the low/mid frequency part is typical of soft van der Waals interactions between adjacent molecules and corresponds to lattice modes (phonons, librons). A gap separates it from the high-frequency modes involving deformations of the molecules shape. In bulk C_{60} crystals, the lattice modes extend up to 8 meV and are separated by a 20 meV gap from the first intramolecular vibration (H_g^1) at 33 meV. The spectrum of the intramolecular modes extends up to about 200 meV (for a review, see Ref. 30). In the solid phase of cubane, the lattice modes extend up to 20 meV (Ref. 31) and the first molecular vibration appears at 76.5 meV.[32] The highest frequency intramolecular modes for the cubane molecule correspond to the C-H stretching modes around 350 meV, which is beyond the energy window of the spectrometer for this experiment.

As explained in Sec. II C, the GDOS of a fullerene-cubane compound originates essentially from modes involving hydrogen displacements, i.e., it is a direct measurement of the partial density of states of hydrogen $g_H(\omega)$. Under ambient conditions, the bonding between the fullerene and the cubane molecules is of van der Waals type. Therefore the intermolecular coupling is weak and the molecular vibrations of cubane are only slightly downshifted from their values in the bulk phase as is observed by Raman spectroscopy.[12] The HF band is therefore dominated by the molecular modes of cubane which are contributing in the (70–190 meV) range in the solid phase. We refer to the work of Yildirim *et al.*[32] who made use of both inelastic neutron scattering and DFT simulations to measure and attribute precisely these vibrations in the case of solid cubane.

In the MF band, a small peak is visible at ~33 meV, in good correspondence with the first C_{60} internal mode of H_g symmetry. The clear observation of this mode in comparison with the other fullerene modes suggests a small hybridization of the H_g fullerene vibrations with other modes involving hydrogen displacements.

The additional intense contributions in the spectrum originate from external degrees of freedom. The primitive cell of the fcc lattice contains one fullerene and one cubane molecule. In the disordered phase, the fullerene molecule can be approximated by a single atom with regards to the external excitations, the rotations being unhindered. Therefore, fullerene and cubane molecules will, respectively, contribute to $3+6=9$ external degrees of freedom, separated into acoustic modes (triply degenerated F_{1u} at Γ point), optical—translational—modes (F_{1u}, OT) and optical—librational—modes (F_{1g}, OL), the latter involving hindered rotations of the cubane molecules around the C_4 axis as required by the O_h symmetry of the lattice and cubane site.

The optical modes are therefore separated into two triply degenerated groups at the Γ point depending on their character (libration OL or translation OT). The librations are weakly dispersive and should contribute as a strong peak to the GDOS. As for the OT modes, the large difference of mass between the cubane and the fullerene molecules $\left[\frac{M(C_{60})}{M(C_8H_8)} \simeq 6.9\right]$ suggests a flat dispersion for these phonon branches as well as a dominant contribution of the cubane components on the polarization vectors for these modes. By contrast, the cubane components of the polarization vectors for the acoustic modes are non-negligible only in the neighborhood of the gamma point (Brillouin zone center) giving almost no contribution to the GDOS for a classical three-dimensional lattice. As a consequence, one expects the observation of two intense contributions (OL and OT) from the external modes of the lattice.

The MF band features two intense peaks at 11 and 17.8 meV (at 300 K) that can be attributed to the above mentioned contributions. They are shown in detail in Fig. 4(a) as a function of temperature, and are compared to MD simulations in the disordered and ordered phases in Fig. 4(b). The temperature evolution shows that whereas the low-energy peak is not affected by the phase transition ($T_c=140$ K), the high energy peak splits into two contributions for temperatures below T_c, with respective integrated intensities in the ratio 1:2 between its low frequency and high-frequency components (located, respectively, at 16.6 meV and 18.3 meV at 100 K).

The use of MD simulations allowed for an easy separation between the modes of translational and rotational character by removing the translational component from the RBT prior to the calculation of the hydrogen GDOS. This gives the two

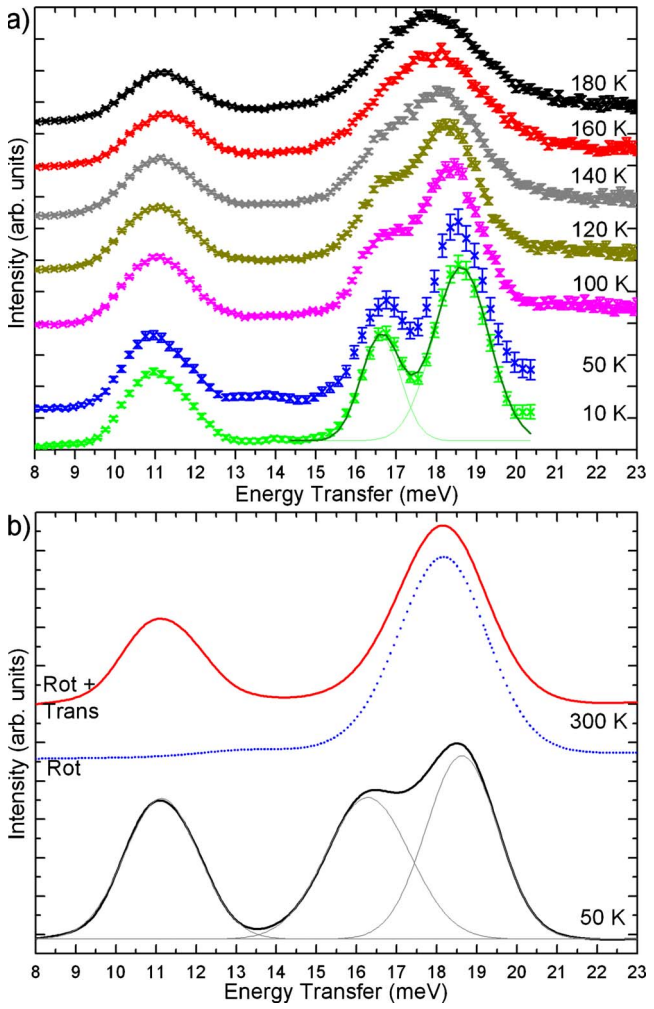

FIG. 4. (Color online) (a) Experimental GDOS at 1.5 Å for temperatures between 180 and 100 K, at 1.65 Å for 50 and 10 K—(b) Simulated GDOS at 180 and 50 K. Simulations were shifted by 1 meV toward low energies. The Rigid Body Trajectory (RBT) allows us to separate translational and rotational motions: the peak at 11 meV is thus due to translations of cubanes, the one at 17.8 meV is due to librations of cubanes (see text).

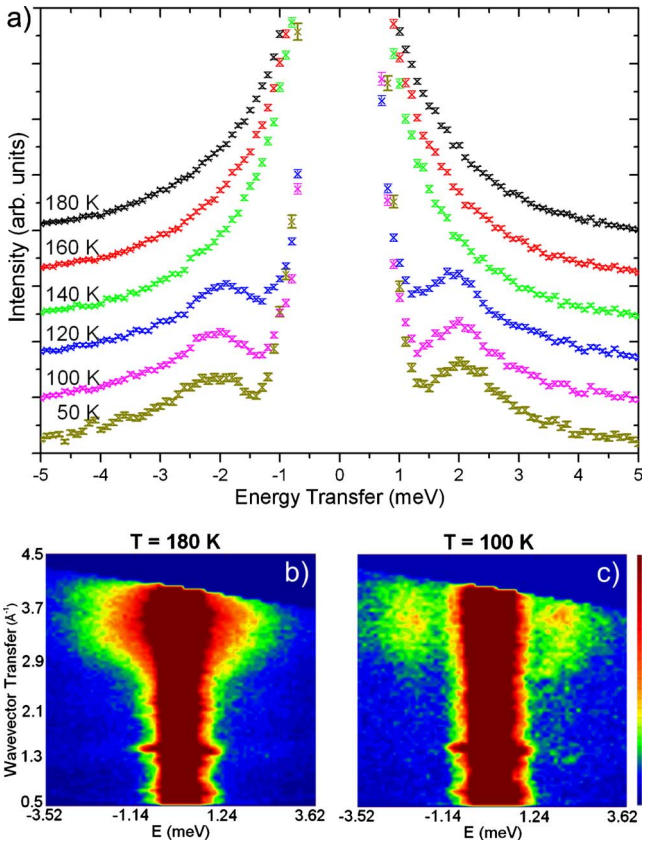

FIG. 5. (Color online) (a) Temperature evolution of the susceptibility $\chi''(\omega)/\omega$ in the LF area (at 2.7 Å) $S(Q,\omega)$ for (b) $T=180$ K and (c) $T=100$ K at 2.7 Å. The Q dependency is the same in both cases and the integrated intensity between 1.3 and 3 meV gives a peak at 3.4 Å^{-1}, which is typical of coherent scattering of fullerenes (Ref. 19).

spectra shown in Fig. 4(b). The full curve labeled rot+trans represents the GDOS calculated at 300 K from RBT containing both rotation and translation degrees of freedom of the molecules. The dashed blue curve, by contrast, represents the GDOS calculated from RBT containing rotational degrees of freedom only. This allows attributing the high-frequency band, observed in both curves, to the librations of the cubane molecule. On this basis, the peaks at 11 and 17.8 meV observed in the experimental data are attributed to the OT and OL contributions, respectively.

The simulations in the *NVE* ensemble reproduce the behavior of the experimental spectra above and below the structural phase transition, with a splitting of the OL feature into two components while keeping the OT peak unchanged. In our simulation, however, the system is still rotor-stator (disordered) down to a temperature of about 100 K, e.g., 40 K lower than observed, and the ratio between the integrated intensity of the low and high-frequency components of the OL peak is different ($\sim 1:1$) from that observed experimentally ($\sim 1:2$). The latter point indicates that the final structure we obtain at low temperature in the simulation is different from that of the real system in its low-temperature ordered phase. The symmetry lowering induced by the phase transition lifts the degeneracy of the librations by breaking the isotropy of the system. The 1:2 ratio shows that two directions in space are equivalent with one differing.

At high temperature, the OL peak in the simulation is Gaussian-type and has an intrinsic broadening, reflecting the statistical distribution of the potential experienced by the cubane molecules when performing small rotations. This is a consequence of the fluctuations of the C_{60} orientations in the disordered phase which are revealed in the low-frequency part of the experimental spectra by the presence of a quasielastic signal (lorentzian broadening of the elastic peak and typical of a diffusive motion) [see Figs. 5(a) and 5(b)]. The Q dependency of the integrated intensity of this quasielastic signal shows a maximum at 3.4 Å^{-1} which is characteristic of C_{60} rotations, analogous to what is observed in their pure crystalline phase.[19] It is well known that this signal, dynamic in nature, is at the origin of the diffuse scattering that is observed as a halo in the diffraction images and discussed in the previous section.

For temperatures below 140 K, the quasielastic signal vanishes in favor of an inelastic peak located at ~2.2 meV. The Q dependency of the intensity of this mode, similar to that of the quasielastic scattering [Fig. 5(b)], is a fingerprint of its librational (rotational) nature. In bulk C_{60} crystal, this order-disorder transition occurs at $T_c=255$ K and the librations are observed at $E_{lib}^{C_{60}} \simeq 2.5$ meV [at 115 K (Ref. 33)]. The librations are therefore softer in the fullerene-cubane compounds and T_c is significantly shifted toward low temperatures. These results are in perfect agreement with recent calorimetric measurements.[15] It is important to note that there is no noticeable evolution of the position of the libration mode when lowering the temperature. In bulk C_{60}, the libration peak upshifts when lowering the temperature down to 90 K below which it remains constant. This shift is associated with a temperature dependent population of the preferential local orientation between adjacent molecules. At 90 K, a glass transition occurs and the system is frozen in a mixture of orientational states. A similar evolution of the peak position is not observed for fullerene cubane.

IV. DISCUSSION

XRDS and INS measurements give a tentative global picture of the fullerene-cubane structure and dynamics. The orthorhombic phase in which $C_{60}\cdot C_8H_8$ crystallizes in the low-temperature ordered phase is a singular case of neutral intercalated C_{60}. First, the simple cubic $Pa\bar{3}$ space group was systematically detected for the O_2C_{60}, N_2C_{60}, ArC_{60}, KrC_{60}, and XeC_{60}, and second, the very high symmetry of the constituent molecules forming the $C_{60}\cdot C_8H_8$ lattice would have made the cubic system a first natural guess. Another interesting peculiarity of this system is the presence of an important disorder in fullerenes' orientations below the transition, in contrast to the expectation in several experimental papers. This disorder is revealed by the observation of a homogeneous diffuse annulus at ~3.3 $Å^{-1}$, not modulated in the ordered phase and equivalent to that in the disordered high temperature phase. In the cubic phase of C_{60}, the merohedral disorder in the low temperature phase leads to a modulation of this annulus. However, these modulations can be smeared out either by dynamical disorder (C_{60} librations) and/or by some residual static disorder, which results from the preponderance of local interaction between the cages.[34,35] For energy integrated techniques, as is the case of XRDS, the discrimination between these two origins is difficult.

Our neutron investigations confirm the rotor-stator nature of the fullerene-cubane system for temperatures higher than 140 K. The high symmetry of the system is highlighted by the presence of a small number of intense peaks in the MF range, attributed to the OT and OL modes. In particular, the OL mode frequency is found at 17.8 meV in the high-temperature phase. Besides, the C_{60} libration peak is observed at 2.2 meV in the low-temperature region. An estimate of the rotational barriers in $C_{60}\cdot C_8H_8$ can be made for both C_{60} and C_8H_8 molecules by assuming that a simple sinusoidal hindrance potential is sufficient to describe their rotational motion. For small amplitudes of libration,

$$E_a = \frac{E_{lib}^2}{B}\left(\frac{\theta}{2\pi}\right)^2 \tag{6}$$

were E_a is the potential barrier, θ is the hopping angle between neighboring potential minima, $B=0.346\times10^{-3}$ meV ($B=14.26\times10^{-3}$) is the rotational constant for C_{60} (C_8H_8) and E_{lib} is the librational energy. Assuming that the reorientational motion for C_{60} follows the scenario proposed by David *et al.* for pure C_{60},[36,37] which supposes ~42° jumps about any one of the three twofold molecular axes that are normal to the ⟨111⟩ direction of the unit cell, one obtains $E_a=180$ meV, which is about 75% the value of the corresponding barrier in the ordered phase of bulk C_{60}.[37] In a recent paper, Matus and co-worker have deduced an activation energy four times smaller from their NMR investigation ($E_a \sim 50$ meV).[38] This suggests that the actual hopping angle between neighboring potential minima for C_{60} is a factor of two smaller ($\theta \sim 21°$) in the $C_{60}\cdot C_8H_8$ than in bulk C_{60}. By contrast, the energy barrier for reorientation around the C_4 axis for cubane is higher by a factor of about 30 ($E_a=1390$ meV). This large difference of energy barrier is responsible for the rotor-stator nature of this system.

Within the quasiharmonic approximation, the mean square angular displacement due to thermal occupation of the librations is given as

$$\langle\theta^2\rangle = \frac{4B}{E_{lib}}\coth\left(\frac{E_{lib}}{2k_BT}\right). \tag{7}$$

At 100 K, this gives a value of $\theta_{rms}=\sqrt{\langle\theta^2\rangle}$ equal to 4.1° for the C_{60} (3.7° for C_8H_8), which gives a corresponding mean square displacement $\langle u^2\rangle_f^{lib}=R^2\langle\theta^2\rangle$ of 0.064 $Å^2$ for the librations of fullerenes, and $\langle u^2\rangle_c^{lib}=0.016$ $Å^2$ for the librations of cubanes (at 180 K, a value of $\langle u^2\rangle_c^{lib}=0.025$ $Å^2$ is found).

These dynamical angular fluctuations are certainly one of the ingredients to explain the structureless XRDS annulus at 3.3 $Å^{-1}$ in the low-temperature phase. It has been shown that the introduction of a $\Delta=3°$ angular dispersion inside the structural model of bulk C_{60} leads to a better description of the modulated XRDS (Ref. 27) in the $Pa\bar{3}$ phase but this dispersion does not smear out the oscillations of the XRDS due to the merohedral disorder. This suggests that the C_{60} orientational disorder revealed by XRDS below 140 K cannot originate from large amplitude librations. We propose that in fullerene-cubane compound, the C_{60} molecules take a larger number of different orientations than in pure C_{60}, corresponding to local energy minima, the fluctuations from these orientations appearing in a time scale much longer than the IN4C resolution. In Ref. 39, Monte Carlo simulations indeed point toward very strong orientational disorder below the transition temperature.

The translational part of the mean-square displacement $\langle u^2\rangle_c^t$ for the cubane molecule can be computed from the value of the frequency of the OT modes, by assuming that the major part of the cubane vibration is contained in this feature. In that case, one can write

$$\langle u^2\rangle_c^t = \frac{\hbar^2}{2M_c E_{OT}} \coth\left(\frac{E_{OT}}{2k_B T}\right) \tag{8}$$

with M_c being the mass of the cubane molecule and E_{OT} =11 meV is the frequency of the OT mode.

We find values of 0.011 and 0.007 Å^2 for the $\langle u^2\rangle_c^t$ at 180 K and 100 K, respectively. This gives a total molecular $\langle u^2\rangle_c = \langle u^2\rangle_c^t + \langle u^2\rangle_c^{lib}$ of 0.035 Å^2 at 180 K (0.024 Å^2 at 100 K) for the cubane molecules. These values are in perfect agreement with the total mean squared displacement obtained from the Q dependency of the intensity of the inelastic peaks, for which we obtain a value of $\langle u^2\rangle_c$ $=0.035\pm0.002$ Å^2 at 180 K and 0.025 ± 0.002 Å^2 at 100 K.

The neutron data reveal that the first-order phase transition at 140 K implies the concomitant blockage of the C_{60} rotation and the lowering of the lattice symmetry, featured by the simultaneous appearance of the libration peak of C_{60} and the splitting of the libration peaks of the C_8H_8. This splitting could reflect the distribution of local environments around the cubane molecule. The 1:2 ratio between intensities of the OL peaks is equal to the ratio between the 30 double bonds (DB) and the 60 single bonds (SB) within a C_{60} molecule. A first attempt to explain this intensity ratio is to suggest that the different local environments could be linked to two different C_{60} orientations associated with a single or a double bond (referred as "SB" and "DB" in the following). Further investigations involving simulations and structural characterizations of the low-temperature phase are required to give more precision on the symmetry of these two states. A step further would be to suggest that the residual disorder in the low-temperature phase could be due to fullerene fluctuations around those preferential orientations and to relaxation by jumps of $\sim 21°$ between them at long time scale, by analogy to what is observed for bulk C_{60} in the $Pa\bar{3}$ phase. However, in the case of $C_{60}\cdot C_8H_8$, we do not observe a strong T dependency of the OL band, nor on the frequency of the C_{60} libration. Within the above hypothesis, this means that the ratio of DB and SB environment is not temperature dependent, suggesting equivalent potential energy for these families but slightly different local curvature.

By contrast to what is observed for the OL modes, the feature associated with the OT modes is constant at all temperatures, being surprisingly unaffected by the transition. This is observed in the experimental data and in the simulated spectra. This indicates first that the behavior of the cubane is harmonic, ruling out the hypothesis of some large – flat – cavity in which the cubane could be oscillating, as proposed by Verberck *et al.*[39] Such "rattling modes" are known to show a very strong temperature dependency as the flatter part of the potential energy surface is dominant at low temperature, giving rise to a downshift of this peak when lowering the temperature, opposite to normal anharmonic behavior.[40,41] And second, this indicates that the transition leads to a change in the local rotational potential energy surface but does not affect noticeably the force constants for translational displacements—thus the "radial" part of the local potential energy surface of the cubane molecules.

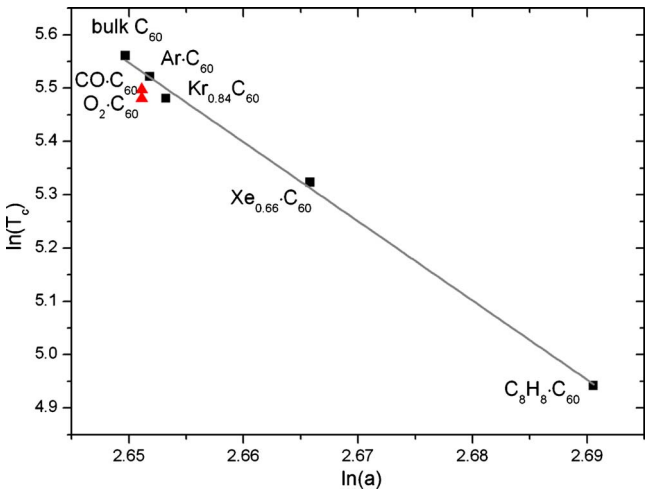

FIG. 6. (Color online) $\ln(T_c^i)$ as a function of $\ln(a)$ at room temperature, as suggested by Ref. 10. T_c^i is the transition temperature for the intercalated compound, a is the corresponding lattice parameter at room temperature. Solid line is a linear fit with values of van der Waals compounds only (squares). Values collected from Refs. 3–7 and 11.

It is well known that intercalating neutral atoms or small molecules influences noticeably the thermodynamics of the fullerene crystal in two ways: (1) downshift of T_c and (2) disappearance of the glass transition. These effects are qualitatively opposite to what is observed when applying pressure, so that they have been qualified as "negative pressure effects." In Fig. 6, we report the evolution of $\ln(T_c)$ as a function of $\ln(a)$, a being the lattice constant of the fcc cell for different cases of intercalated molecules AC_{60}. We observe that the cubane point lies on a line extrapolating the point for inert gases. This linear dependence allows to extract a Grüneisen-type parameter[42] $\gamma = -\frac{\partial(\ln T_c)}{\partial(\ln a)}$ which measures the strength of the $T_c(a)$ dependence, i.e., the fractional change in T_c over a fractional change in a. A value of γ=22.8 was found when applying pressure[10] while we find γ $=14.8\pm0.2$ in this study. This indicates a softer dependence in the case of intercalation.

V. CONCLUSION

We have used XRDS and INS to shed light on the structure and dynamics of the $C_{60}\cdot C_8H_8$ cocrystal in the low-temperature phase. XRDS studies showed that a homogeneous diffuse halo is still visible below the transition, meaning that an important disorder still remains in fullerenes' orientations below T_c.

The INS measurements presented in this work confirm that the room temperature phase is rotor-stator by the direct observation of the quasielastic signal of the fullerene. The

rotor-stator phase undergoes an order/disorder transition below 140 K, in which the fullerenes' orientations are frozen, highlighted by the appearance of inelastic features attributed to the libration modes of the fullerene at $E_{lib}^{FC}=2.2$ meV. The external modes of the cubane molecules are clearly observed: the OT mode is measured at 11 meV and the libration appears as a single line in the disordered phase at 17.8 meV. This band is split into two peaks at 16.6 and 18.3 meV (at 100 K) with an intensity ratio 1:2 below the transition. We tentatively attribute each of these two peaks to a peculiar local environment of the cubane, the low energy one being associated to a "DB" configuration and the high frequency one to a "SB" configuration—each configuration being associated to a specific orientation of the adjacent C_{60}. We ruled out that dynamical disorder is at the origin of the homogeneity of the diffuse halos observed in the XRDS picture in the low-temperature phase and proposed that this disorder is from "static" origin.

The determination of the orientations of fullerenes and the position of cubanes in the low-temperature phase is a prerequisite to better understand this rich system.

ACKNOWLEDGMENTS

The authors acknowledge P.-A. Albouy and S. Rouzière (LPS, Orsay) for fruitful discussions and for their support during diffuse scattering experiments. Work in Hungary was supported by the Hungarian Research Fund, OTKA under Grant No. K72954. The CS group at the ILL is acknowledged for their support during the MD simulations.

[1] M. Riccò, M. Belli, M. Mazzani, D. Pontiroli, D. Quintavalle, A. Jánossy, and G. Csányi, Phys. Rev. Lett. **102**, 145901 (2009).
[2] A. Ganin, Y. Takabayashi, Y. Khimyak, S. Margadonna, A. Tamai, M. Rosseinsky, and K. Prassides, Nature Mater. **7**, 367 (2008).
[3] F. Yan, Y.-N. Wang, and M. Gu, J. Phys.: Condens. Matter **10**, 6875 (1998).
[4] B. Renker, H. Schober, M. T. Fernandez-Diaz, and R. Heid, Phys. Rev. B **61**, 13960 (2000).
[5] M. Gu, T. B. Tang, C. Hu, and D. Feng, Phys. Rev. B **58**, 659 (1998).
[6] S. van Smaalen, R. Dinnebier, W. Schnelle, I. Holleman, G. von Helden, and G. Meijer, Europhys. Lett. **43**, 302 (1998).
[7] G. Gadd *et al.*, J. Phys. Chem. Solids **58**, 1823 (1997).
[8] P. Heiney, J. Phys. Chem. Solids **53**, 1333 (1992).
[9] F. Gugenberger, R. Heid, C. Meingast, P. Adelmann, M. Braun, H. Wühl, M. Haluska, and H. Kuzmany, Phys. Rev. Lett. **69**, 3774 (1992).
[10] G. A. Samara, J. E. Schirber, B. Morosin, L. V. Hansen, D. Loy, and A. P. Sylwester, Phys. Rev. Lett. **67**, 3136 (1991).
[11] S. Pekker, E. Kovats, and G. Faigel, Nature Mater. **4**, 764 (2005).
[12] G. Klupp, F. Borondics, E. Kovats, A. Pekker, G. Benyei, I. Jalsovszky, R. Hackl, S. Pekker, and K. Kamaras, J. Phys. Chem. B **111**, 12375 (2007).
[13] A. Iwasiewicz-Wabnig, B. Sundqvist, E. Kovats, I. Jalsovszky, and S. Pekker, Phys. Rev. B **75**, 024114 (2007).
[14] M. Bokor, P. Matus, P. Banki, G. Kriza, K. Tompa, E. Kovats, S. Pekker, G. Benyei, and I. Jalsovszky, Phys. Status Solidi B **245**, 2010 (2008).
[15] N. M. Nemes, M. Hernandez, G. Bortel, E. Kovats, B. Nagy, I. Jalsovszky, and S. Pekker, J. Phys. Chem. B **113**, 2042 (2009).
[16] V. Coluci, F. Sato, S. Braga, M. Skaf, and D. Galvao, J. Chem. Phys. **129**, 064506 (2008).
[17] P. Eaton and T. Cole, J. Am. Chem. Soc. **86**, 3157 (1964).
[18] Resolutions are given at elastic scattering and energy ranges are expressed considering the down scattering (Stokes) side only, i.e., the energy range accessible at the lowest temperature.
[19] D. A. Neumann *et al.*, Phys. Rev. Lett. **67**, 3808 (1991).
[20] H. Schober, A. Tölle, B. Renker, R. Heid, and F. Gompf, Phys. Rev. B **56**, 5937 (1997).
[21] M. Bée, *Quasielastic Neutron Scattering* (Adam Hilger and Bristol, Philadelphia, 1988).
[22] P. Launois, S. Ravy, and R. Moret, Phys. Rev. B **52**, 5414 (1995).
[23] http://accelrys.com/products/materials-studio/
[24] http://dirac.cnrs-orleans.fr/plone/software/nmoldyn/
[25] B. Verberck, V. Heresanu, S. Rouzière, J. Cambedouzou, P. Launois, E. Kováts, S. Pekker, G. Vliegenthart, K. Michel, and G. Gompper, Fullerenes, Nanotubes, Carbon Nanostruct. **16**, 293 (2008).
[26] P. Launois, S. Ravy, and R. Moret, Int. J. Mod. Phys. B **13**, 253 (1999).
[27] R. Moret, P. Launois, S. Ravy, M. Julier, and J. Godard, Synth. Met. **86**, 2327 (1997).
[28] A. Marucci, P. Launois, R. Moret, and A. Penicaud, Eur. Phys. J. B **26**, 29 (2002).
[29] P. Launois, R. Moret, N.-R. de Souza, J. Azamar-Barrios, and A. Pénicaud, Eur. Phys. J. B **15**, 445 (2000).
[30] L. Pintschovius, Rep. Prog. Phys. **59**, 473 (1996).
[31] P. Gehring, D. Neumann, W. Kamitakahara, J. Rush, P. Eaton, and D. VanMeurs, J. Phys. Chem. **99**, 4429 (1995).
[32] T. Yildirim, S. Ciraci, C. Kilic, and A. Buldum, Phys. Rev. B **62**, 7625 (2000).
[33] J. Copley, D. Neumann, R. Cappelletti, and W. Kamitakahara, J. Phys. Chem. Solids **53**, 1353 (1992).
[34] S. L. Chaplot, L. Pintschovius, M. Haluska, and H. Kuzmany, Phys. Rev. B **51**, 17028 (1995).
[35] O. Blaschko, G. Krexner, C. Maier, and R. Karawatzki, Phys. Rev. B **56**, 2288 (1997).
[36] W. I. F. David, R. M. Ibberson, T. J. S. Dennis, J. P. Hare, and K. Prassides, Europhys. Lett. **18**, 735 (1992).
[37] J. Copley, W. David, and D. Neumann, Neutron News **4**, 20 (1993).

[38] P. Matus, M. Bokor, G. Kriza, É. Kováts, S. Pekker, A. Domján, G. Durkó, and I. Jalsovszky, Phys. Status Solidi B **246**, 2764 (2009).

[39] B. Verberck, G. Vliegenthart, and G. Gompper, J. Chem. Phys. **130**, 154510 (2009).

[40] H. Schober, H. Itoh, A. Klapproth, V. Chihaia, and W. Kuhs, Eur. Phys. J. E **12**, 41 (2003).

[41] S. Rols, H. Jobic, and H. Schober, C. R. Phys. **8**, 777 (2007).

[42] The Grüneisen parameter $\gamma_j(\vec{k}) = -\frac{\partial[\ln \omega_j(\vec{k})]}{\partial(\ln V)}$ represents the relative change in the frequency of the oscillator as a function of the volume of the system. For more information on this subject, the lector can refer to N. W. Ashcroft and N. D. Mermin, *Solid State Physics* (Saunders College, Philadelphia, 1976), Chap. 25.